Desalination and Water Treatment
www.deswater.com
doi: 10.5004/dwt.2023.30105

314 (2023) 35–48
December

Manufacturing of cost-effective sorbent from by-product materials for treating real and simulated groundwater contaminated with antibiotics

Layla Abdulkareem Mokif*, Ayad A.H. Faisal

Department of Environmental Engineering, College of Engineering, University of Baghdad, IQ-BG, 10071, Baghdad, Iraq, emails: laila.mukheef2011d@coeng.uobaghdad.edu.iq (L.A. Mokif), ayad.faesal@coeng.uobaghdad.edu.iq (A.A.H. Faisal)

Received 21 August 2023; Accepted 29 October 2023

ABSTRACT

A novel adsorbent is synthesized from chicken bone wastes to support attempts to reuse them. To prepare the nanoparticles of calcium-iron oxide, the calcium ions have been extracted from chicken bones and combined with iron ions under specific conditions. Sodium alginate is used to immobilize the nanoparticles through synthesizing calcium/iron oxide - sodium alginate beads employed for tetracycline (TC) antibiotic adsorption. Batch experiments are conducted at a contact time of 0–180 min, initial TC concentration of 100–250 mg/L, agitation speed of 50–250 rpm, initial pH of 3–12, and beads dosage of 0.1–1.3 g/50 mL. The best vales for batch parameters are 90 min, 100 mg/L, 200 rpm, 7, and 1.3 g/50 mL, respectively. These conditions enable the beads to remove 97.116% of TC with 8 mg/g as maximum capacity. The precise formulation of the kinetic observations by the pseudo-second-order model indicates that the TC could be eliminated by chemical forces. The characterization tests provide evidence that nanoparticles formed inside the beads can support the sorption of TC, especially the particles that mainly consist of calcium-iron oxide. The beads are capable of removing TC from real groundwater with an efficiency smaller than that in the aqueous solution due to the presence of various chemicals.

Keywords: Nanoparticle; Calcium-iron oxide; Tetracycline; Antibiotic; Wastewater treatment; Adsorption

1. Introduction

Together with the issue of water scarcity, water pollution has emerged as a major global concern. It is common knowledge that industry and agriculture consume the most water. These economic sectors are expected to consume an exponential amount of water in the coming years, which will have a negative impact on the reserves and quality of freshwater. In this regard, the world's emerging economy necessitates the implementation of novel planning for the entire transition of the linear economy of the present to a brand-new notion depending on the keeping and regrowth of natural capital. As a result, the sustainable management of water represents a continual challenge, especially due to a number of parameters including the expanding global population, depletion of water resources, and, last but not least, an expanding global demand for clean water, bioenergy, and food. Hence, the removal of pollutants and decontamination of the pollutant source requires rapid and efficient actions [1–4]. Nowadays, controlling pollution has grown to be a top priority for the society, since there are numerous reasons for water pollution [5]. In industrial wastewater, there are several types of contaminants such as pharmaceuticals, dyes, phenols, pesticides, hydrocarbons, heavy metals, and others. Every nation's economy depends heavily on the pharmaceutical sector because pharmaceuticals are so essential to survival and are so valuable. Numerous pharmacologically active components are recognized in wastewater, surface-water, and groundwater at levels that are detrimental to environmental safety. Also, the

* Corresponding author.

presence of pharmaceuticals at trace levels in the water cycle and ambient environment (in the range from nano-grams to micrograms per liter) has been widely explored and published in the literature over the last decade [6,7]. Antibiotics are among the medications with a high potential for harm to the environment and reach the ambient not only through the emissions from pharmaceutical and chemical industries but also primarily through livestock and sewage, as between 25% and 75% of ingested medications are ejected in unchanged shape after passage in the gastro-intestinal tract [8].

Tetracycline (TC) is the most widely used antibiotic worldwide. TC is produced by actinomycetes and is effective against the gram-negative and the gram-positive bacteria in addition to a board of bacterial illnesses. Tetrahydrobenzene derivatives having a dibasic tetraphenyl base structure are known as TC. Tetracycline antibiotics are composed mostly of TC, oxytetracycline, and chlortetracycline [9]. Because of its widespread usage in agriculture, livestock, human disease prevention, and TC contamination is becoming an increasing global hazard to terrestrial and aquatic biodiversity [10].

Tetracycline's excessive usage by humans and animals, along with its poor capacity to decompose, has made it a severe environmental danger. Tetracycline may accumulate in the food chain, be hazardous to the microbial population, promote the emergence and spread of antibiotic resistance, endanger the safety of irrigation and drinking water, and alter the ecology of the bacteria in the human intestine [11]. Tetracycline contamination in the aquatic environment is mostly caused by the overuse of this antibiotic in human and animal medicine and its usage in agriculture as a growth promoter [12]. Hospitals, the pharmaceutical sector, household sewage, and livestock farming are the main sources of TC and all contribute to the buildup of TC in wastewater systems [13]. Tetracycline consumption by humans globally is about 23 kg/d [14]. Each year, Britain manufactures 438 tons of antibiotics, of which 228 tons, or 52% of the total, are produced as TCs. The production of TCs in China, which accounts for 46% of all antibiotic output, is estimated to be 97,000 tons [15].

Antibiotic concentrations in the aquatic environment have been removed using a variety of approaches, including biological treatment and membrane technology, coagulation–flocculation, advanced oxidation processes, artificial wetlands, and adsorption [16–19]. The physico-chemical properties of the tetracycline, the properties of the sorbent, and the environmental variables, such as temperature and the presence of other chemicals, all affect the degree and rate of the degradation process. Due to adsorption and desorption, leaching, drainage, absorption by crops, dispersion, and volatilization, the tetracycline may migrate from one phase to another throughout the degradation process in the aquatic environment. Additionally, during this transportation via transformation mechanisms like hydrolysis, photocatalytic degradation, bioremediation, oxidation, and reduction, the structure of TC may change to a different structure [20].

Adsorption is an effective method that has proven its efficiency in comparison to other treatments of wastewater [21–23]. This technique has numerous benefits; specifically [24,25]: (i) it used to treat hazardous metals and organic species; (ii) its adaptability in design and operation; (iii) the needed area is smaller than a biological system's. Accordingly, many adsorbents like clay minerals, wastes of bark, peat, fly ash, byproducts generated from available industries, wood powder, sludge of metal hydroxide, and agricultural wastes, can be used to remediate the water polluted with various kinds of chemical species [26]. Due to applications of nanoparticles (NPs) in specialized fields including medicine, cancer theranostics, biosensing, catalysis, agriculture, and the environment, magnetic nanoparticles (MNPs) in particular can be utilized as good sorbents for removing of chemicals in wastewater remediation because of their low-cost, higher surface area, and stability [27,28]. Alginate has valuable advantages due to its cheapness and its ease of forming cross-linking with the solution of $CaCl_2$ [29]. Calcium cations are capable of binding two carboxyl moieties of guluronic residues in the alginate chains. It is a natural product that can be considered inexpensive, biodegradable, non–toxic, biocompatible, and water-soluble. It has been widely applied for the immobilization of nanoparticles of TiO_2, carbon nanotubes, activated carbon, and magnetite generating novel sorbents to eliminate chemicals from wastewater [30]. The use of composite materials for pollutant adsorption has been suggested to be more effective than other methods due to their low-cost, simple design, accessibility, and ability to capture pollutants [31].

Numerous materials used for TC adsorption such as [Fe(III)@CNFs] dealing with the endothermic adsorption of TCs and four adsorption mechanisms were found including surface complexation between TC and Fe(III), electrostatic interaction, hydrogen bonding, and van der Waals force [32]. Tetracycline antibiotics can be extracted from an aqueous solution using graphene oxide (GO), which has the potential to be an efficient sorbent and it was strongly deposited on the GO surface by cation-π bonding and π–π interaction [33]. In tap water, river water, and pharmaceutical effluent, the Cu-ZIF-8 adsorbent presented remarkable adsorption performance toward TC, chemical adsorption was predominant in the interaction of TC with Cu-ZIF-8. Cu-ZIF-8 adsorption surface was uniform, according to adsorption kinetics and isotherms analyses. Also, the adsorption of TC over Cu-ZIF-8 was exothermic and spontaneous, according to adsorption thermodynamics [34]. The electrostatic interaction and ion exchange of NH_2 groups and COOH on MIL-88A/g-C_3N_4 to TC are the most important mechanisms by which TC is adsorbed on MIL-88A/g-C_3N_4 [35]. The TC adsorption occurred on the external surface of raw bentonite as well as in the interlayer region, and it was controlled by both chemical and physical mechanisms [36]. The adsorption efficiency of Z-HAP-AA-1:3 was assessed in relation to the initial TC concentration 50–400 mg/L, temperature 30°C–50°C, and pH 3–13 during removing TC in a batch procedure. The data were most accurately represented by the Freundlich model. The highest monolayer adsorption capacities of Z-HAP-AA for tetracycline were, respectively, 186.09, 212.56, and 244.63 mg/g at 30°C, 40°C, and 50°C [37].

In addition to the significant contamination of the water supply, the planet faces the problem of an increasing amount of municipal solid waste (MSW) production, which is seriously contaminating groundwater sources and soils [38,39]. Annually, the meat industry generates large quantities of

bone waste reaching millions of tons worldwide. Reports from the Organization for Economic Cooperation and Development (OECD) state that meat production is expected to rise by 40 million tons in the next few years, with 13% of that growth coming from poultry meat. As a result, global production of waste meat and bone meal will significantly rise [40]. Bone contains both organic and inorganic components. The main constituent of the inorganic part of the bone is crystalline salt minerals in the form of calcium phosphate compounds, which are frequently known as hydroxyapatite. Researchers face a great challenge in converting such raw wastes into nonconventional and effective sorbents for eliminating chemicals from polluted water [41–43].

As a result, the novel aspect of the present research is to extract calcium from the wastes of chicken bones which can be prepared in large amounts from poultries, restaurants, homes, and food industrialization units. However, the calcium ions can be reacted with iron to synthesize calcium-iron oxide nanoparticles through precipitation, followed by the use of sodium alginate to immobilize these particles as beads. The particular objectives of this research are: (i) synthesizing the novel adsorbent called the beads of (calcium/iron oxide) - sodium alginate; (ii) investigating the efficacy of these beads in the capturing of TC from an aqueous environment; (iii) identifying the suitable conditions for suitable touch between prepared beads and adopted antibiotic. The objectives can be accomplished by combining characterization investigations, and batch experiments, with the formulation of experimental measurements by equilibrium and kinetic models.

2. Materials and method

2.1. Chemicals and materials

In this research, TC antibiotic was the target contaminant. The stock solution of TC was prepared at room temperature. The pH adjustment was performed by drops of 0.1 M NaOH and HCl. For detecting the TC concentrations, a UV-visible spectrophotometer with a model of (Shimadzu UV-1900i, Japan) can be utilized and the reading must be taken at a wavelength of 357 nm [44,45]. Immobilization of calcium/iron oxide nanoparticles can be achieved through the application of sodium alginate (molecular weight of 2.5×10^5 g/mol, Sigma-Aldrich, USA).

2.2. Manufacturing of (calcium/iron oxide) - sodium alginate beads

The wastes of chicken bones had been collected from household waste and local restaurants. These wastes had been soaked into hot water and washed with distilled water (DW) to detach residual fat and the impurities; then, the wastes must be grinded for obtaining certain distribution of particle sizes. For the extraction purposes of calcium ions, a specific amount of chicken bone wastes had been added to an amount of 300 mL aqueous solution consisting of DW and a certain concentration of hydrochloric acid (HCl %). The mixture must agitate using a magnetic stirrer for 3 h at ambient temperature. The aqueous solution enriched with calcium ions could be separated from the residual waste particles using the Whatman No. 1 filter paper. The process of preparation requires dissolving a certain mass of $FeCl_3$ in DW to obtain an aqueous solution of iron ions. It is necessary to mix the two solutions of calcium and iron together with various molar ratios of concentrations. Nanoparticles of calcium/iron oxides can be obtained through the precipitation method by changing the acidity of the mixture [46].

Various values of pH 7, 8, 10, and 12 were used by adding 1 M NaOH to the mixture for obtaining an optimum value of the acidity needed for synthesizing calcium/iron oxide nanoparticles. The mixture must be stirred till approaching the occurrence of heavy brownish precipitates which can be separated using filter papers and then they must be dried at a temperature of 85°C overnight. These dried materials had been rinsed several times with DW for removing impurities and after that they had been annealed for 8 h at a temperature of 200°C and then grinded manually for producing nanoparticles powder of calcium/iron oxide. For synthesizing beads of (calcium/iron oxide) - sodium alginate, an amount of sodium alginate of 2 g should be dissolved in one hundred milliliters of DW and the solution resulting from this process should be stirred via a magnetic stirrer for 24 h at ambient temperature. The produced nanoparticles of calcium/iron oxide had been mixed in different amounts with a solution sodium alginate. For bead composing and polymerization, the produced slurry had been added into a solution of $CaCl_2$ with 0.1 M by means of 10 mL syringe. The beads had been dried at 105°C with diameters of (3–4) mm [47]. Fig. 1 depicts in details the steps of accomplishing the experimental work in the present study for preparing the beads of (calcium/iron oxide) - sodium alginate. The efficiency of TC removal is considered as the indicator used to determine the satisfactory conditions, solution's pH, (Ca/Fe) molar ratio, and dosage of calcium-iron oxide NPs that had been required for the synthesizing process.

Several analyses were performed to assess the sorbent characteristics. Alginate beads and calcium-iron oxide nanoparticles have undergone X-ray diffraction (XRD) analysis in order to identify the crystalline form. The XRD was measured using the XRD Siemens model, D500, TGA-DSC: STA500, (Germany). Fourier-transform infrared spectroscopy (FTIR) was employed to determine the functional groups on the surface of the sorbent using Jasco 4200, Japan. The scanning electron microscopy-energy-dispersive X-ray spectroscopy (SEM-EDS) analysis was examined using the ZEISS model: Sigma VP, EDS, and mapping: Oxford Instruments, UK.

3. Batch experiments

Through a series of batch studies, the kinetic and equilibrium of TC adsorption onto (calcium/iron oxide) - sodium alginate beads have been investigated. These studies are designed to identify the appropriate values of initial pH, agitation speed, time, initial concentration (C_0), and bead mass that necessary to remove the most molecules of adopted antibiotic for selected C_0. Several flasks have been prepared, and each flask contains an amount of the simulated polluted water (V) of 50 mL with a specific C_0. Polluted water was combined with various masses of prepared beads (m) within the flasks that must agitate for 3 h at 200 rpm. After

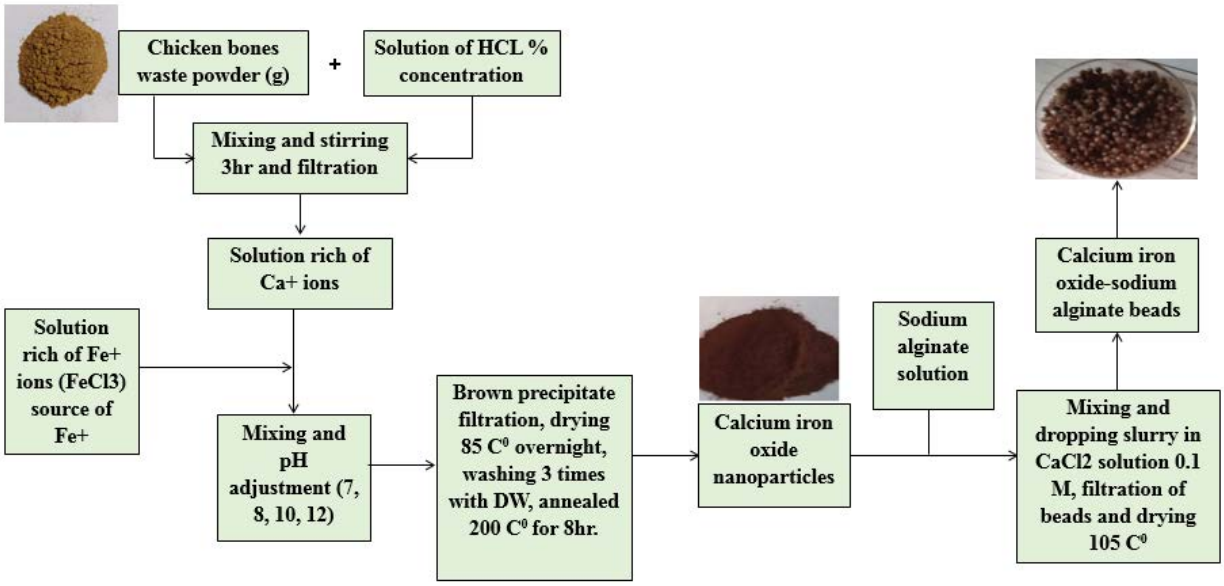

Fig. 1. Flow chart for preparation of (calcium/iron oxide) - sodium alginate beads used in this work.

finishing each test, the produced beads must be isolated from the water by means of filter paper, and the concentration of TC at equilibrium (C_e) may be evaluated by a UV spectrophotometer. Eq. (1) is applied in the estimation of the TC quantity retained on the beads at the equilibrium (q_e) based on the differential between C_e and C_0. The conditions of batch experiments were C_0 of TC (100–250 mg/L), pH (3–12), time (5–180) min, agitation speed (50–250) rpm, and dosage of beads (0.1–1.3) g/50 mL. Eq. (2) can be employed to compute the TC removal percentage (R%) [48].

$$q_e = \frac{\left(C_0 - C_e\right)V}{m} \tag{1}$$

$$R\left(\%\right) = \frac{C_0 - C_e}{C_0} \times 100 \tag{2}$$

4. Sorption data modeling

4.1. Equilibrium sorption isotherm

Mathematically, adsorption is defined using an equilibrium isotherm model that relates concentrations of chemical's residues attached to the solid particles in water at the equilibrium for certain temperature. The adsorption isotherm model [Eq. (3)] [49] used in this research is represented by the Langmuir model which is applied to determine the highest sorption capacity (q_{max}, mg/g) corresponding to the prepared sorbent.

$$q_e = \frac{q_{\max} b C_e}{1 + bC_e} \tag{3}$$

where b represents the sorbent particles - contaminant molecules affinity (L/mg).

4.2. Kinetic models

The contaminant transfer rate from the aqueous solution to solid particles is very important to the design of a proper sorption process [50]. Over the last two decades, the majority of adsorption kinetic investigations have utilized the two conventional models listed in Eqs. (4) and (5) for the formulation of kinetic datasets. These models are used in a wide range of adsorption systems, including biomass and nanomaterials as adsorbents, as well as heavy metals and medicines as contaminants.

- Pseudo-first-order model: is popular formula [Eq. (4)] applied to describe the rate of solute sorption [51]:

$$q_t = q_e\left(1 - e^{-k_1 t}\right) \tag{4}$$

where k_1 represents the rate constant for this model (1/min). The parameters q_t and q_e (mg/g) are the amounts of solute retained on the sorbent particles at time t and the equilibrium state, respectively.

- Pseudo-second-order model: assumes that a single layer of the solute adheres to the sorbent particles, that the sorption energy cannot vary for each sorbent, and that there is no sign of interaction between the sorbed chemicals. It is written as in Eq. (5) [52]:

$$q_t = \frac{k_2 q_e^2 t}{\left(1 + k_2 q_e t\right)} \tag{5}$$

where k_2 refers to the rate constant for second-order model (g/mg·min).

- Intraparticle diffusion model: is developed by Weber–Morris:

$$q_t = k_{int} t^{0.5} + C \quad (6)$$

where k_{int} refers to the rate constant for the diffusion model (mg/g·min$^{0.5}$) and the intercept value can be illustrated by C [53].

5. Results and discussion

5.1. Calcium extraction

The extraction process of the calcium ions from the wastes of chicken bones requires considering two affecting factors which are the effect of the hydrochloric acid concentration (HCl %) and the amount of bone wastes as illustrated in Fig. 2. To identify the appropriate concentration of HCl, 20 g of the chicken bone's waste was added to 300 mL of solution composed of DW concentrated with 4%, 6%, and 10% of hydraulic acid. However, the results of these tests are depicted in Fig. 2a. This figure certifies that the higher acid percentage can extract more quantity of calcium ions and the highest concentration of Ca (=6,317 mg/L) can possibly be determined at a greater percentage of HCl (=10%). For specifying the best amount of bone waste that should be employed, the wastes of 20 to 140 g had been added to 300 mL of a solution consisting of 10% of HCl and the outcomes are explained in Fig. 2b. It is obvious that the increase of waste mass from 20 to 120 g can associate with a remarkable increase in the concentration of calcium ions extracted from such waste with a range from 6,317 to 44,218 mg/L. Hence, 10% HCl and 140 g of chicken bone's waste can be used to obtain greater values of calcium concentration that is used in the preparation of the present sorbent.

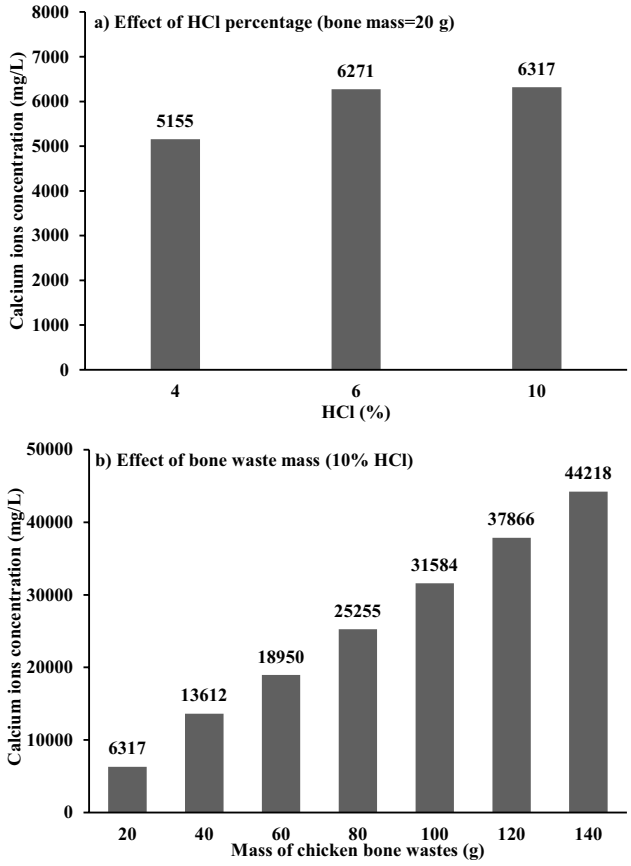

Fig. 2. Extraction of calcium ions from chicken bones wastes under the effects of (a) HCl percentage and (b) mass of bone wastes.

5.2. Manufacturing of alginate beads

The pH of (Ca/Fe) solution, molar ratio, and the nanoparticles mass of calcium/iron are adopted as the prime parameters that affect synthesizing (calcium/iron oxide) - sodium alginate beads. The attained greatest efficiency for eliminating TC from wastewater can be the suitable indicator for selecting the suitable magnitudes for the parameters of synthesis. The pH impact on the bead's preparation had been calculated in the extent from 7 to 12 and measurements can be illustrated in Fig. 3a for (Ca/Fe) of 1, and calcium/iron nanoparticles dosage of 1 g/100 mL. For this figure, the sorption tests are conducted with a bead mass of 0.5 g/50 mL, initial pH of 7, and C_o of 100 mg/L for a contaminated solution, and speed of 200 rpm for a contact time of 3 h. The maximum removal efficiency for TC of 38.77% occurred at pH 10; however, the values of efficiencies at pH 7, 8, and 12 were 20.34%, 27.30%, and 36.18%, respectively.

The second group of experiments was conducted at pH 10 at the same nanoparticle's dosage adopted previously with changing the ratio of Ca to Fe in the range from 0.5 to 4. The outcomes of these sorption tests, conducted under the same operational conditions as those used to investigate the impact of pH, are depicted in Fig. 3b. It seems that the maximum removal (38.77%) can occur at molar ratio 1; however, the increase or decrease in the value of this ratio from 1 can be accompanied with a remarkable decrease in the removal percentage. The last parameter examined in the formation of alginate beads was the nanoparticle dosage of (calcium/iron oxide) through the stabilization of pH and (Ca/Fe) ratio at the best values specified previously. Fig. 3c proves that the TC removal can increase due to the variation of nanoparticle mass from 1 to 5 g and the highest removal can be detected at a dosage of 5 g.

5.3. Characterization of beads

The analysis via XRD had been exploited to determine the patterns of diffraction corresponding to the beads which were prepared from the oxides of iron and calcium with 2θ values starting from 10° to 80°. Such an analysis validated the formation of the nanoparticles produced from calcium-iron oxide. The phase identification process of calcium-iron oxide is carried out by the search and match process using the X'Pert HighScore Plus Software (Version 3). Fig. 4a illustrates the XRD profile for the crystalline composition of alginate beads. Numerous diffraction reflections were identified as shown in Fig. 4a. The active sites in the alginate beads that are capable of removing TC out of an aqueous solution are depicted by these reflections.

The FTIR spectra corresponding the produced beads before and after the sorption of TC are plotted in Fig. 4b taking into account the primary functional groups which are enhancing antibiotic adsorption. This figure showed

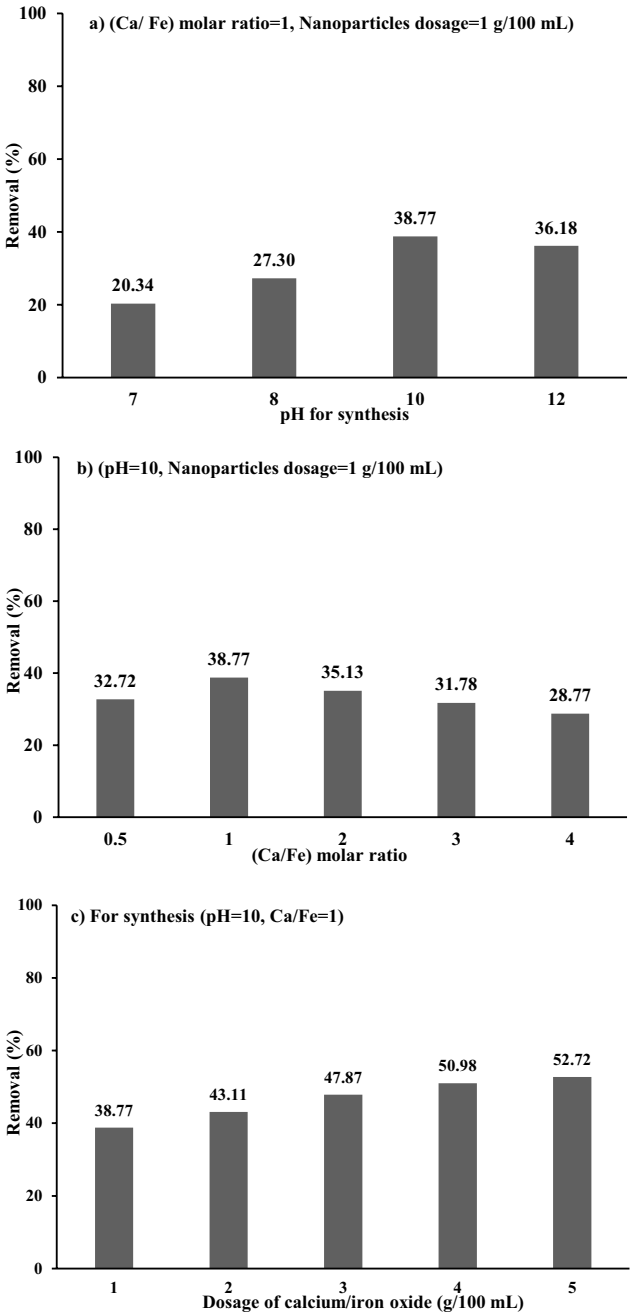

Fig. 3. Conditions for synthesis of alginate beads that used for sorption of tetracycline from wastewater at pH 7, beads dosage 0.5 g/50 mL, speed 200 rpm, time 3 h, and C_o = 100 mg/L. (a) Ca/Fe) molar ratio = 1, nanoparticles dosage = 1 g/100 mL, (b) pH = 10, nanoparticles dosage = 1 g/100 mL, and (c) for synthesis (pH = 10, Ca/Fe = 1).

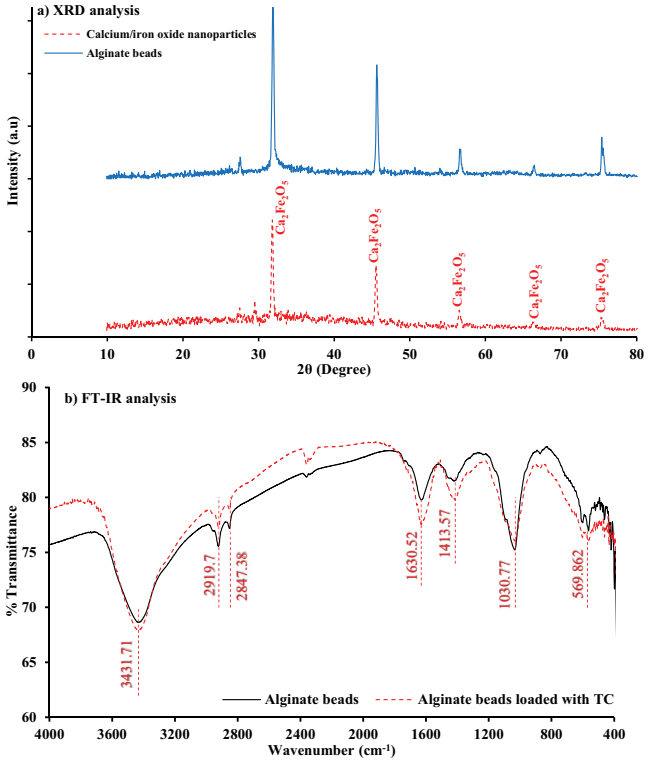

Fig. 4. (a) X-ray diffraction outcomes for crystalline compositions of calcium/iron oxide nanoparticles and (b) Fourier-transform infrared spectroscopy profile for prepared beads after and before tetracycline adsorption.

that amides with (–OH) groups have experienced stretching vibrations that result in absorption bands of high-intensity to form. The peaks for alginate beads have demonstrated a strong and broad absorption band at a frequency band of 3,550–3,200 cm^{-1} which was induced via the stretching vibration of the hydrogen bonds in addition to stretching mode of OH groups. Peaks at 3,431.71; 2,924.52 and 2,847.38 cm^{-1} correspond to OH and C–H stretching vibrations, respectively. The 1,628.51 and 1,418.39 cm^{-1} peaks correspond to the stretching vibrations of O–H and –COO-(symmetric), respectively. To some extent, the weak bands taking place at 1,033 cm^{-1} have been associated to C–O stretching of C–O–H and COO– groups [54]. Stretching vibrations of Fe–O including ferrite skeleton in addition to Ca–O bonds correspond to the bands of absorption at 309.228, 442, and 564.077 cm^{-1} [55,56].

SEM graphs can be used to describe the morphological characteristics of produced beads after and before contact with tetracycline, as illustrated in Fig. 5a and b. The mean rod particle is shown in Fig. 5a and this figure shows that the prepared sorbent's porous surfaces have nonhomogeneous morphology at 200 nm magnification scales. The surfaces might be incredibly compact and disordered. The beads' surface appears to be macroporous, allowing oxyanions to be absorbed. There are noticeable morphological changes in the beads following the removal of TC when compared to the sorbent before the sorption process. Graphs of EDS may be used to characterize the magnitude of change detected in the elemental percentages of the alginate beads composition beyond the process of sorption shown in Fig. 5c & d and Table 1. This table describes the extraordinary rise in *C* content that occurs after TC sorption, which validates the adsorption of such antibiotics.

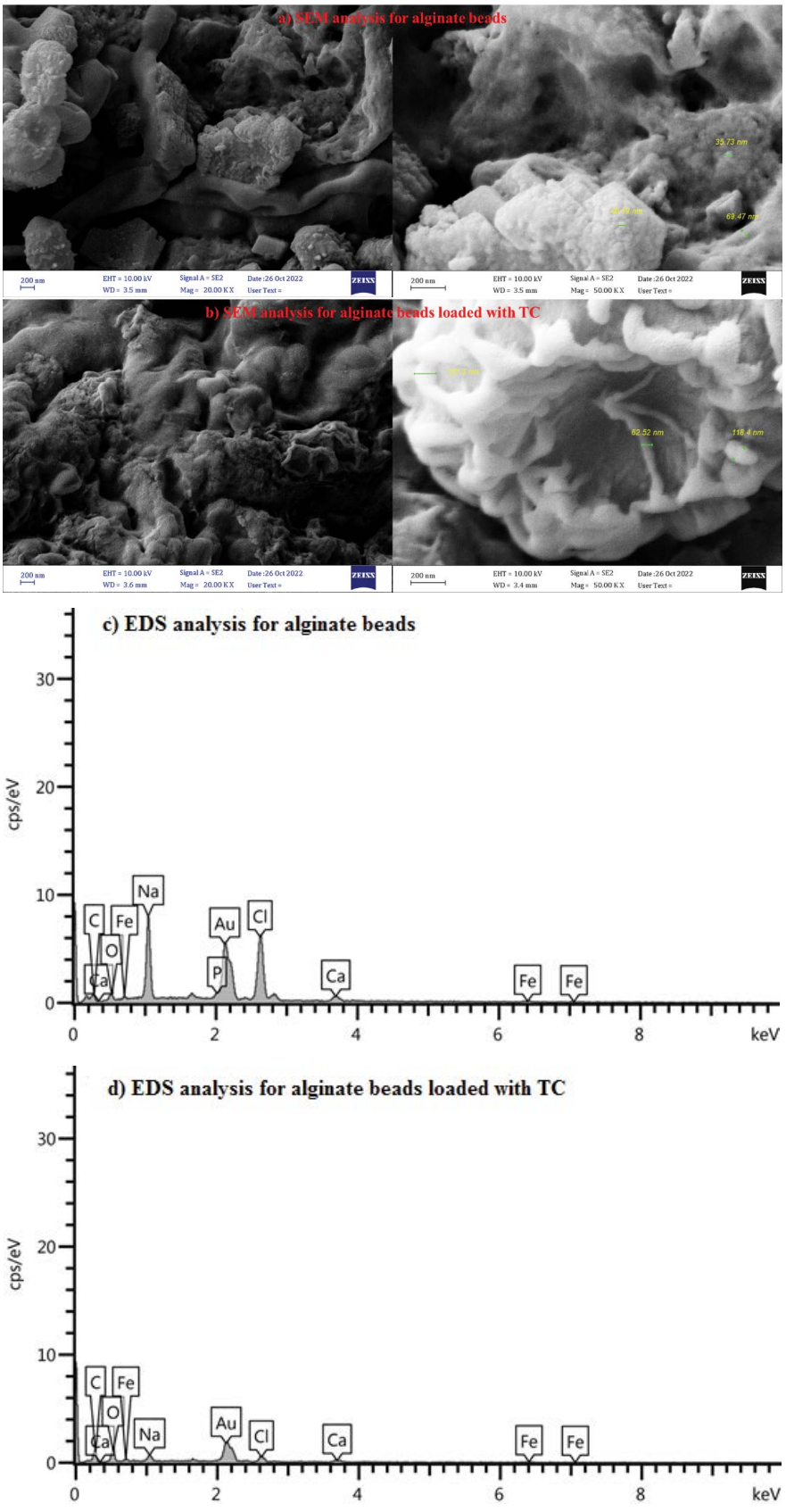

Fig. 5. Scanning electron microscopy and energy-dispersive X-ray spectroscopy graphs for calcium/iron oxide - sodium alginate beads before and after adsorption of tetracycline antibiotic.

Table 1
Elemental percentages in the prepared beads before and after sorption of TC as computed energy-dispersive X-ray spectroscopy analysis

Element (%)	Alginate beads	Alginate beads loaded with TC
C	6.6	30.6
Na	23.7	7.1
Ca	10.5	8.1
Fe	15.6	4.3
Cl	22.3	11.5
O	18.7	14.7
P	2.2	0

5.4. Batch experiments

5.4.1. Contact time

The crucial step in determining the contaminants distributed between the sorbent and solution phases in batch research is the time that must be achieved in the equilibrium condition. The change in TC adsorption efficiency for contact times up to 180 min at C_o 100 mg/L, beads dosage of 0.5 g/50 mL, pH 7, and agitation speeds of 200 rpm is plotted in Fig. 6a. The tetracycline antibiotic is removed at a high rate at the beginning of the test, and the rate can be reduced after 90 min because of the decrease in the vacant sites [57,58]. The findings show that the TC sorption efficacy was 51.52% at 90 min; however, there is no notable increase in the removal percentages beyond this time till 180 min.

5.4.2. Initial concentration of TC

Fig. 6b illustrates that the removal efficiencies of TC are affected greatly by the C_o of adopted antibiotics. These efficiencies were significantly lowered, from 51.52% to 38.88% as a result of to vary of C_o from 100 to 250 mg/L, respectively at 90 min, pH 7, sorbent dosage of 0.5 g/50 mL, and a speed of 200 rpm. At lower concentrations, it is anticipated that all TC molecules will interact with the available binding sites, which will undoubtedly result in a notable increment in the efficiency of sorption; however, a high number of contaminant molecules due to an increase in concentration with specific grams of beads may result in a decrease in this efficiency [59,60].

5.4.3. Agitation speed

A significant factor in the improvement of TC removal is the speed of agitation. Fig. 6c depicts the effect of agitation speed on removal effectiveness. It is observed that when agitation speed increased, the removal efficiency of TC increased. In fact, the high agitation speed accelerates the diffusion of pollutants through alginate beads, allowing for the development of appropriate interaction between the contaminant and the sites of binding. Additionally, the results showed that an agitation speed of 200 rpm was sufficient to ensure maximum TC uptake, and there is no obvious change in the removal after this value.

5.4.4. Initial pH

The solution acidity affects the charge of the bead's surface, ionization degree, and the functional group dissociation; accordingly, it is considered as a prime factor in the sorption of TC from an aqueous solution. Tetracycline's charges vary with solution pH; when the pH is below 4, the protonation of the dimethyl ammonium group causes TC to transform into a cation (TCH^{+1}). Tetracycline becomes a zwitterion (TCH_2^0) at pH 3.5–7.5 as a result of the phenolic diketone moiety losing a proton. Tetracycline becomes an anion (TCH^- or TC^{-2}) at pH levels higher than 7 as a result of the loss of protons from the tri-carbonyl system and phenolic di-ketone moiety [61]. The removal efficiencies of TC are plotted vs. various initial pH values, ranging from 3 to 12, as illustrated in Fig. 6d. The removal efficiency of TC was low (31.99%) at pH 3.0 because the H^+ ions can compete with molecules of this antibiotic. The sorption efficiency may be shown to improve clearly as pH moves closer to neutral, reaching values of at least 51.52% at pH 7. At neutral conditions, the antibiotic's hydration and ionization can decrease, which can speed up the sorption by enhancing the π–π stacking effect and hydrogen bonding. When the pH is close to neutral, TC molecules are zwitterions, and as the pH rises, increases the density of their negative charge. It is hypothesized that the alginate beads and TC are most attracted to one other when the neutral pH is compatible with the highest uptake of TC at pH 7.0. The deprotonated adsorbent will produce electrostatic repulsion with the protonated TC when pH is more than 7, which reduces the adsorption performance. This results from the OH ions generation which led to the attenuation in the bonding of hydrogen [62].

5.4.5. Point of zero charge (pH_{pzc})

The pH at which the sorbent surface is neutral is known as the point of zero charge. This means that the positive and negative charges have equal amounts. The surface has positive charges for pH below this point; otherwise, the surface will be having negative charges. The ionization mechanism of functional groups and the pattern of their interactions with chemical compounds in the solution can be hypothesized using this phenomenon. By using the solid addition method, the pH_{pzc} of the adopted sorbent can be calculated, and this value can be used to explain the removal process. This method included the preparation of ten conical flasks that were filled with a solution of NaCl (0.01 M) with various values of pH ranging from 3 to 12, the dosage of beads 0.5 g, and the mixture must agitate for 48 h at 200 rpm. At the end of the test, the final values of pH were measured and the difference in pH between final and initial values of pH (ΔpH) must be plotted with initial pH as expressed in Fig. 6e. It is clear that the pH_{pzc} has a value of 7 which leads to the highest removal of TC antibiotic. The prepared adsorbent had positive charges at pH below 7 and negative charges at pH above 7.

5.4.6. Adsorbent dosages

The impacts of beads grams on the TC sorption were examined in the range from 0.1 to 1.3 g per 50 mL of solution

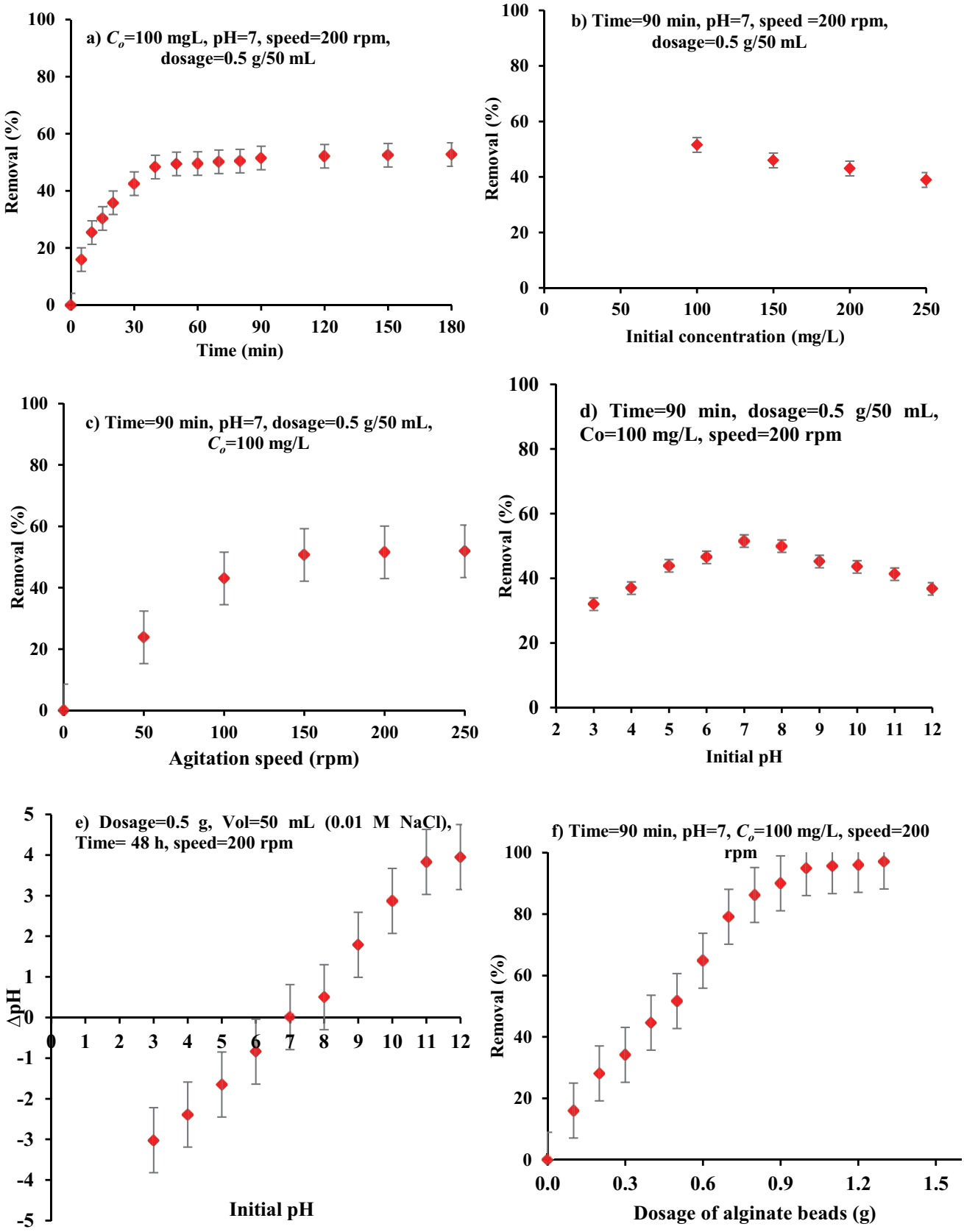

Fig. 6. Influences of (a) time, (b) initial concentration, (c) agitation speed, (d) initial pH of solution, (e) point of zero charge and (f) adsorbent dose on the prepared adsorbent behavior employed to remove TC from contaminated aqueous solution.

in order to identify the optimum dose. According to Fig. 6f, the TC removal efficiency can increase with higher mass of the beads. This may be explicated by the fact that as alginate beads dosage increased, the effective areas and the sites number increased [63]. The removal efficiency ranged from 16.01% at 0.1 g to 97.116% at the adsorbent mass of 1.3 g and the best dosage can be adopted at 1 g/50 mL.

5.5. Sorption kinetics

By "The Solver Tool in Microsoft Excel 2016", kinetic outcomes for the change of sorbed tetracycline vs. experiment time were fitted using non-linear regression with Eqs. (5) and (6). The constants for models of kinetic obtained in the fitting process are introduced in Table 2. The sum of squared error (SSE) and determination coefficient (R^2) must be calculated to characterize the agreement degree between mentioned models and experimental data, which can be seen in Fig. 7a and Table 2. According to values of R^2 = 0.974 and SSE = 0.531, the pseudo-second-order model is more practical for illustrating the sorption of TC onto prepared beads. Additionally, the calculated value of TC sorbed quantity (q_e) is very close to the measured value (that is equal to 5.491 mg/g) and this is another sign of the suitability of the pseudo-second-order model to represent such measurements. Accordingly, chemical forces may be the prime cause for the elimination of adopted contaminants from aqueous solutions. The values of k_1 and k_2 are used to indicate how quickly the adsorption equilibrium is reached. According to previous studies, the rate constants are always inversely proportional to the solute's initial [64,65]. The present findings proved that the value of k_2 is less than that of k_1 which means the sorption reaction between TC and beads needs more time to reach the equilibrium.

Eq. (6) in conjugation with Fig. 7b signifies the intraparticle diffusion role in the TC elimination. This figure demonstrates that the q_t and $t^{0.5}$ are related by linear relation; as a result, when the line passes in the origin, this diffusion should occur and serve as the rate-limiting process. Table 1 lists the constants of this linear that were computed via linear fitting. However, it appears that the intercept for this curve does not equal zero, indicating that there will be additional processes operating in addition to intraparticle diffusion. Three regions constitute the linear plot; the first one is sharper and governed by the instantaneous or external surface sorption; however, the second and third regions can be changed gradually [66]. Using the Langmuir model; the maximum sorption capacity of TC is 8 mg/g, indicating that alginate beads have efficient capability of removing TC antibiotic. Table 3 shows the current research outcome in comparison with TC's sorption capacities and removal efficiencies for various materials from the available literature.

Table 2
Kinetic variables for tetracycline antibiotic sorption onto alginate beads

Model	Factor	Value
Pseudo-first-order	q_e (mg/g)	5.076
	k_1 (min^{-1})	0.0741
	R^2	0.968
	SSE	0.755
Pseudo-second-order	q_e (mg/g)	5.881
	k_2 (min^{-1})	0.0133
	R^2	0.974
	SSE	0.531
Intraparticle diffusion	Region 1	
	k_{int} (mg/g·min$^{0.5}$)	0.777
	R^2	0.996
	Region 2	
	k_{int} (mg/g·min$^{0.5}$)	0.0873
	R^2	0.940
	Region 3	
	k_{int} (mg/g·min$^{0.5}$)	0.0306
	R^2	0.975

5.6. Desorption kinetics

For evaluating an adsorbent's potential and efficacy, the desorption properties must be investigated. With 50 mL of water containing 100 mg/L of TC, 0.5 g of alginate beads

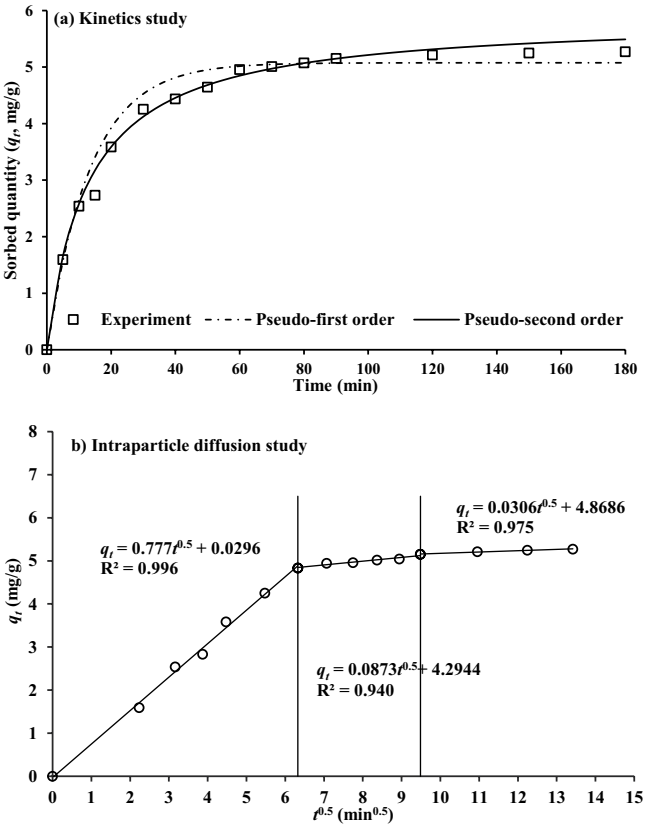

Fig. 7. Kinetic models for sodium alginate beads interaction with water contained TC molecules (symbols: experimental measurements and lines; fitted models). (a) Kinetics study and (b) intraparticle diffusion study.

Table 3
Current research outcome in comparison with TC's sorption capacities for various materials from available literature

Sorbent	q_{max} (mg/g)	Removal efficiency (R %)	References
Graphene oxide-magnetic particles	18.3	98%	[67]
Hydroxyapatite/pumice composites	17.87	86%	[68]
$MnFe_2O_4$/rGO nanocomposite	41	–	[69]
Re-generable pumice	3.345	80%	[70]
Cobalt oxide	0.023	≥20	[61]
α-Fe_2O_3/rGO	9.69	–	[71]
Nano-magnetic walnut shell-rice husk	7.283	–	[72]
Geo-materials	10	–	[45]
Hydroxyapatite coated filter cake	43.534	≥95%	[73]
(Ca/Fe)-LDH-sodium alginate	10.393	≥95%	[47]
$Ca_2Fe_2O_4$–Na alginate beads	8	97.11%	This study

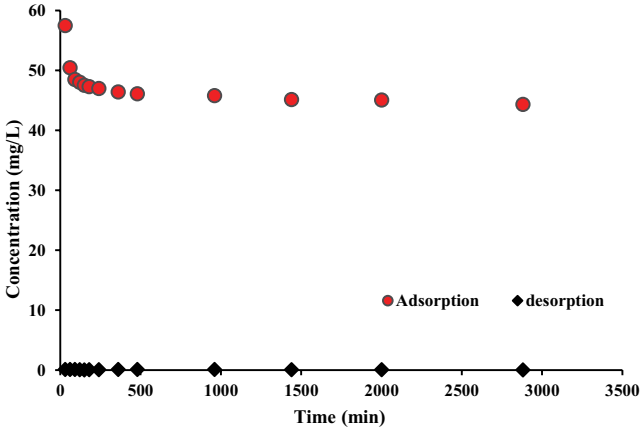

Fig. 8. Desorption outputs for (calcium/iron oxide) - sodium alginate beads.

was utilized. Adsorption outcomes at pH 7, 200 rpm, and a contact time extension of 2,880 min are presented in Fig. 8. The desorption tests were also carried out using deionized water as the washing agent because it is a practical choice to determine the amount of TC desorbed from the sorbent loaded with TC. Results are shown in Fig. 8 where TC concentrations in the washing solution for a duration of up to 2,880 min have values no more than 0.0211 mg/L. These outcomes certified the reliability of the prepared sorbent in the containment of contaminant molecules for a long duration of time; consequently, the exhausted beads can be landfilled in sanitary locations.

5.7. Prepared beads for the removal of TC from real groundwater

The efficiency of prepared beads in the treatment of groundwater samples contaminated with TC was examined. The groundwater samples were collected from local wells within the boundaries of Babylon Governorate-Iraq. Table 4 lists the characteristics of the collected groundwater and it is obvious that the values of total dissolved salts and total hardness are very high. The interaction of beads and real groundwater is tested under the variation of time, sorbent dosage, and initial concentration to evaluate the adsorbent's efficacy in the capturing of TC from such water. The adsorbent mass values were 0.1, 0.3, 0.5, 0.7, 1.1, and 1.3 mg/L, while the TC concentrations have been implemented with values of 100, 150, 200, and 250 mg/L for a time ranging from 30 to 180 min at an agitation speed of 200 rpm. Fig. 9 presents a comparison between the treatment efficacies of beads in the remediation of groundwater and prepared solutions contaminated with TC. The results revealed that the effectiveness of the adsorbent in the case of groundwater was less than that observed in the case of a simulated solution prepared in the laboratory. The difference in efficiencies may result from the presence of organic and inorganic constituents in the groundwater that will compete with the TC molecules to occupy the vacant sites of beads.

Table 4
Characteristics of real groundwater investigated in the current work

Parameter	Value
pH	7.4
Turbidity (NTU)	11.2
Total dissolved salts (mg/L)	4,062
Total suspended solids (mg/L)	18.4
ALK (mg/L)	286
Total hardness (mg/L)	2,760
Tetracycline (mg/L)	0

6. Conclusions

This study developed a novel adsorbent successfully prepared from natural by-product wastes in order to remove tetracycline from contaminated water. Calcium ions were effectively extracted from chicken bones that must mix with iron ions to form nanoparticles of calcium/iron oxide through the precipitation process. The chicken bones are produced in large quantities as solid waste and its utilization can represent an effective application feasible for sustainable subjects. The prepared nanoparticles-alginate beads

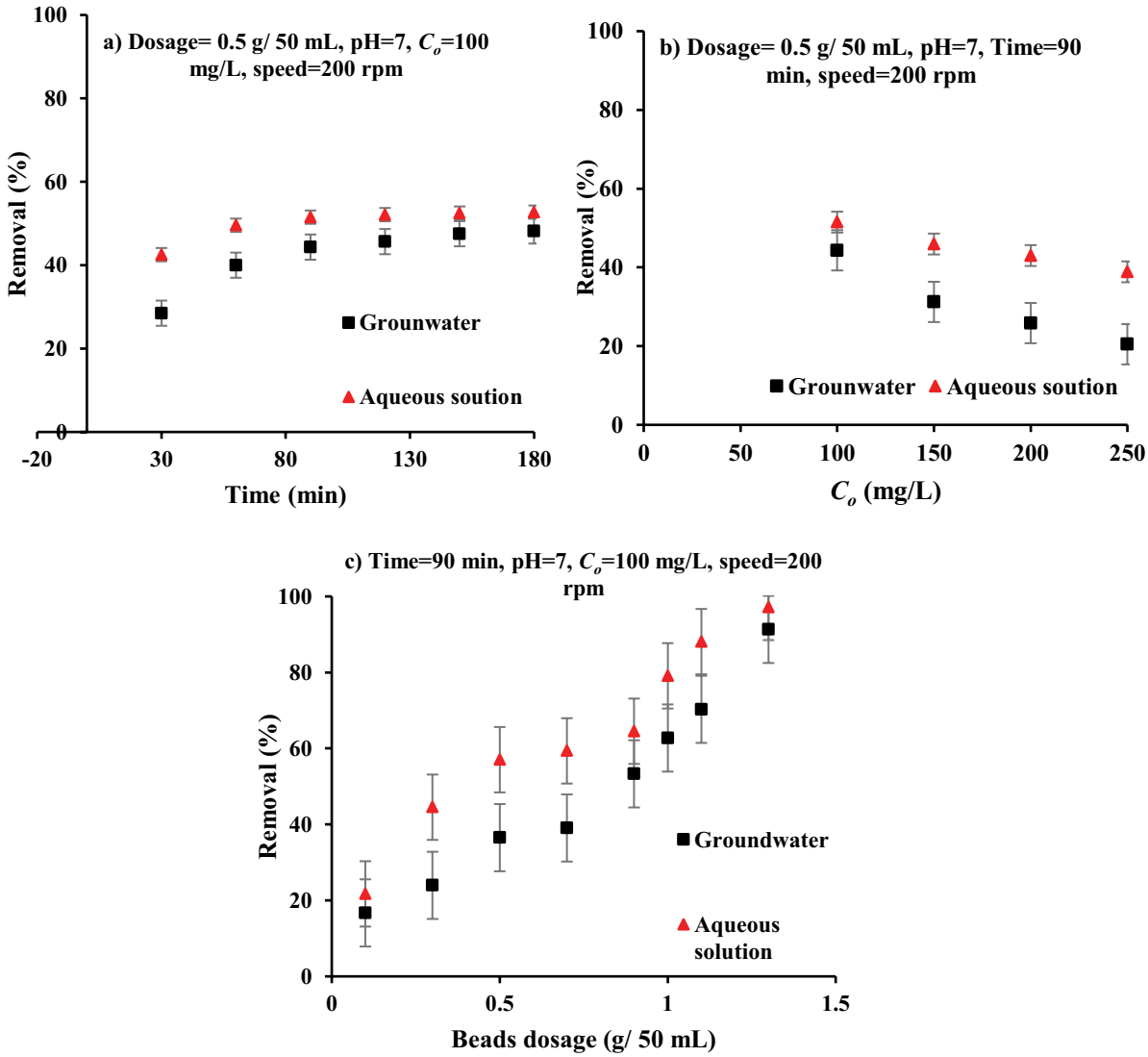

Fig. 9. Comparison between efficacy of adsorbent in the remediation of real groundwater and simulated solution contaminated with TC vs. (a) time, (b) sorbent mass, and (c) initial concentration.

have spherical shapes and batch tests were implemented to determine the ability of such beads in the removal of TC from simulated and real groundwater. The maximum sorption capacity for prepared alginate beads was 8 mg/g as calculated from the Langmuir equilibrium model. The application of a pseudo-second-order model on kinetic data means the chemical forces, or chemisorption are governed by the TC removal. The prepared beads' characterization tests demonstrated the nanoparticle's formation of calcium-iron oxide. The main recommendation for the present study is to find the ability to use the prepared beads in the permeable reactive barrier technique which considers the in-situ method for remediating contaminated groundwater.

References

[1] P. Ghisellini, C. Cialani, S. Ulgiati, A review on circular economy: the expected transition to a balanced interplay of environmental and economic systems, J. Cleaner Prod., 114 (2016) 11–32.

[2] A.A.H. Faisal, Z.S. Nassir, Modeling the removal of cadmium ions from aqueous solutions onto olive pips using neural network technique, Al-Khwarizmi Eng. J., 12 (2016) 1–9.

[3] H. Rashid, A. Faisal, Removal of dissolved trivalent chromium ions from contaminated wastewater using locally available raw scrap iron-aluminum waste, Al-Khwarizmi Eng. J., 15 (2019) 134–143.

[4] A.A. Ibrahim, M.A. Ibrahim, A.G. Yusuf, Implications of industrial effluents on surface water and ground water, World J. Adv. Res. Rev., 9 (2021) 330–336.

[5] M. Jerold, K. Vasantharaj, C. Vigneshwaran, V. Sivasubramanian, Evaluation of biosorption potential of *Gracilaria corticata* for the removal of malachite green from aqueous solution: isotherm, kinetic and thermodynamic studies, Desal. Water Treat., 66 (2017) 251–262.

[6] A. Babatunde, E.P. Bamgbola, O. Oyelola, The effect of pharmaceutical effluents on the quality of groundwater: a case study of Ikeja industrial area of lagos, Nigeria, Int. J. Res. Med. Health Sci., 4 (2014).

[7] M. Kumar, A. Gogoi, D. Kumari, R. Borah, P. Das, P. Mazumder, V.K. Tyagi, Review of perspective, problems, challenges, and future scenario of metal contamination in the urban environment, J. Hazard. Toxic Radioact. Waste, 21 (2017) 4017007, doi: 10.1061/(ASCE)HZ.2153-5515.0000351.

[8] A.A. Borghi, M.S.A. Palma, Tetracycline: production, waste treatment and environmental impact assessment, Braz. J. Pharm. Sci., 50 (2014) 25–40.
[9] F. Granados-Chinchilla, C. Rodríguez, Tetracyclines in food and feedingstuffs: from regulation to analytical methods, bacterial resistance, and environmental and health implications, J. Anal. Methods Chem., 2017 (2017) 1–24.
[10] F. Ahmad, D. Zhu, J. Sun, Environmental fate of tetracycline antibiotics: degradation pathway mechanisms, challenges, and perspectives, Environ. Sci. Eur., 33 (2021) 64, doi: 10.1186/s12302-021-00505-y.
[11] Y. Amangelsin, Y. Semenova, M. Dadar, M. Aljofan, G. Bjørklund, The impact of tetracycline pollution on the aquatic environment and removal strategies, Antibiotics, 12 (2023) 440, doi: 10.3390/antibiotics12030440.
[12] L. Xu, H. Zhang, P. Xiong, Q. Zhu, C. Liao, G. Jiang, Occurrence, fate, and risk assessment of typical tetracycline antibiotics in the aquatic environment: a review, Sci. Total Environ., 753 (2021) 141975, doi: 10.1016/j.scitotenv.2020.141975.
[13] P. Mahamallik, S. Saha, A. Pal, Tetracycline degradation in aquatic environment by highly porous MnO_2 nanosheet assembly, Chem. Eng. J., 276 (2015) 155–165.
[14] V.J. Wirtz, A. Dreser, R. Gonzales, Trends in antibiotic utilization in eight Latin American countries, 1997–2007, Rev. Panam. Salud Publica/Pan Am. J. Public Health, 27 (2010) 219–225.
[15] Y. Dai, M. Liu, J. Li, S. Yang, Y. Sun, Q. Sun, W. Wang, L. Lu, K. Zhang, J. Xu, W. Zheng, Z. Hu, Y. Yang, Y. Gao, Z. Liu, A review on pollution situation and treatment methods of tetracycline in groundwater, Sep. Sci. Technol., 55 (2020) 1005–1021.
[16] M.S. de Ilurdoz, J.J. Sadhwani, J.V. Reboso, Antibiotic removal processes from water & wastewater for the protection of the aquatic environment - a review, J. Water Process Eng., 45 (2022) 102474, doi: 10.1016/j.jwpe.2021.102474.
[17] Y. Zhang, Y.-G. Zhao, F. Maqbool, Y. Hu, Removal of antibiotics pollutants in wastewater by UV-based advanced oxidation processes: Influence of water matrix components, processes optimization and application: a review, J. Water Process Eng., 45 (2022) 102496, doi: 10.1016/j.jwpe.2021.102496.
[18] M.M. Barbooti, S.H. Zahraw, Removal of amoxicillin from water by adsorption on water treatment residues, Baghdad Sci. J., 17 (2020) 1071, doi: 10.21123/bsj.2020.17.3(Suppl.).1071.
[19] W.A. Khanday, M.J. Ahmed, P.U. Okoye, E.H. Hummadi, B.H. Hameed, Single-step pyrolysis of phosphoric acid-activated chitin for efficient adsorption of cephalexin antibiotic, Bioresour. Technol., 280 (2019) 255–259.
[20] I.T. Carvalho, L. Santos, Antibiotics in the aquatic environments: a review of the European scenario, Environ. Int., 94 (2016) 736–757.
[21] Mu. Naushad, Z.A. Alothman, M.R. Awual, M.M. Alam, G.E. Eldesoky, Adsorption kinetics, isotherms, and thermodynamic studies for the adsorption of Pb^{2+} and Hg^{2+} metal ions from aqueous medium using Ti(IV) iodovanadate cation exchanger, Ionics (Kiel), 21 (2015) 2237–2245.
[22] W.A. Khanday, M. Asif, B.H. Hameed, Cross-linked beads of activated oil palm ash zeolite/chitosan composite as a bio-adsorbent for the removal of Methylene Blue and Acid Blue 29 dyes, Int. J. Biol. Macromol., 95 (2017) 895–902.
[23] F. Marrakchi, W.A. Khanday, M. Asif, B.H. Hameed, Cross-linked chitosan/sepiolite composite for the adsorption of Methylene Blue and Reactive Orange 16, Int. J. Biol. Macromol., 93 (2016) 1231–1239.
[24] A.A.H. Faisal, T.R. Abbas, S.H. Jassam, Iron permeable reactive barrier for removal of lead from contaminated groundwater, J. Eng., 20 (2014) 29–46.
[25] M. Faisal, A. Ahmed, Remediation of groundwater contaminated with copper ions by waste foundry sand permeable barrier, J. Eng., 20 (2014) 62–77.
[26] S. Sonal, A. Singh, B.K. Mishra, Decolorization of reactive dye Remazol Brilliant Blue R by zirconium oxychloride as a novel coagulant: optimization through response surface methodology, Water Sci. Technol., 78 (2018) 379–389.
[27] M. Goodarz Naseri, E.B. Saion, A. Kamali, An Overview on nanocrystalline $ZnFe_2O_4$, $MnFe_2O_4$, and $CoFe_2O_4$ synthesized by a thermal treatment method, ISRN Nanotechnol., 2012 (2012) 1–11.
[28] A. Abedini, A. Rajabi, F. Larki, M. Saraji, M.S. Islam, Structural, magnetic and mechanical properties of hydrous Fe/Ni-based oxide components nanoparticles synthesized by radiolytic method, J. Alloys Compd., 711 (2017) 190–196.
[29] N.P. Raval, S. Mukherjee, N.K. Shah, P. Gikas, M. Kumar, Hexametaphosphate cross-linked chitosan beads for the eco-efficient removal of organic dyes: tackling water quality, J. Environ. Manage., 280 (2021) 111680, doi: 10.1016/j.jenvman.2020.111680.
[30] S. Lilhare, S.B. Mathew, A.K. Singh, S.A.C. Carabineiro, Calcium alginate beads with entrapped iron oxide magnetic nanoparticles functionalized with methionine—a versatile adsorbent for arsenic removal, Nanomaterials, 11 (2021) 1345, doi: 10.3390/nano11051345.
[31] R. Sivashankar, A. Thirunavukkarasu, R. Nithya, J. Kanimozhi, A.B. Sathya, V. Sivasubramanian, Sequestration of methylene blue dye from aqueous solution by magnetic biocomposite: three level Box–Behnken experimental design optimization and kinetic studies, Sep. Sci. Technol., 55 (2020) 1752–1765.
[32] L. Lu, M. Liu, Y. Chen, Y. Luo, Effective removal of tetracycline antibiotics from wastewater using practically applicable iron(III)-loaded cellulose nanofibres, R. Soc. Open Sci., 8 (2021) 210336, doi: 10.1098/rsos.210336.
[33] Y. Gao, Y. Li, L. Zhang, H. Huang, J. Hu, S.M. Shah, X. Su, Adsorption and removal of tetracycline antibiotics from aqueous solution by graphene oxide, J. Colloid Interface Sci., 368 (2012) 540–546.
[34] S. Sun, Z. Yang, J. Cao, Y. Wang, W. Xiong, Copper-doped ZIF-8 with high adsorption performance for removal of tetracycline from aqueous solution, J. Solid State Chem., 285 (2020) 121219, doi: 10.1016/j.jssc.2020.121219.
[35] S. Zheng, Z. Kong, L. Meng, J. Song, N. Jiang, Y. Gao, J. Guo, T. Mu, M. Huang, MIL-88A grown in-situ on graphitic carbon nitride (g-C_3N_4) as a novel sorbent: synthesis, characterization, and high-performance of tetracycline removal and mechanism, Adv. Powder Technol., 31 (2020) 4344–4353.
[36] U. Ortiz-Ramos, R. Leyva-Ramos, E. Mendoza-Mendoza, A. Aragón-Piña, Removal of tetracycline from aqueous solutions by adsorption on raw Ca-bentonite. Effect of operating conditions and adsorption mechanism, Chem. Eng. J., 432 (2022) 134428, doi: 10.1016/j.cej.2021.134428.
[37] W.A. Khanday, B.H. Hameed, Zeolite-hydroxyapatite-activated oil palm ash composite for antibiotic tetracycline adsorption, Fuel, 215 (2018) 499–505.
[38] M. Alhendal, M.J. Nasir, K.S. Hashim, J. Amoako-Attah, D. Al-Faluji, M. Muradov, P. Kot, B. Abdulhadi, Cost-effective hybrid filter for remediation of water from fluoride, IOP Conf. Ser.: Mater. Sci. Eng., 888 (2020) 012038, doi: 10.1088/1757-899X/888/1/012038.
[39] A.K. Alenezi, H.A. Hasan, K.S. Hashim, J. Amoako-Attah, M. Gkantou, M. Muradov, P. Kot, B. Abdulhadi, Zeolite-assisted electrocoagulation for remediation of phosphate from calcium-phosphate solution, IOP Conf. Ser.: Mater. Sci. Eng., 888 (2020) 012031, doi: 10.1088/1757-899X/888/1/012031.
[40] S.S.A. Alkurdi, R.A. Al-Juboori, J. Bundschuh, I. Hamawand, Bone char as a green sorbent for removing health threatening fluoride from drinking water, Environ. Int., 127 (2019) 704–719.
[41] C.M.F. Santos, C.M. Narciso, I.R. Soares, Analysis of heat treatment of chicken bones for the obtaining of phosphate biofertilizer, Braz. J. Dev., 6 (2020) 14288–14296.
[42] W.S.B. Dwandaru, E.K. Sari, Chicken bone wastes as precursor for C-dots in olive oil, J. Phys. Sci., 31 (2020) 113–131.
[43] A.-E. Segneanu, C.N. Marin, G. Vlase, C. Cepan, M. Mihailescu, C. Muntean, I. Grozescu, Highly efficient engineered waste eggshell-fly ash for cadmium removal from aqueous solution, Sci. Rep., 12 (2022) 9676, doi: 10.1038/s41598-022-13664-6.
[44] C. Wang, J.-J. Jian, Degradation and detoxicity of tetracycline by an enhanced sonolysis, J. Water Environ. Technol., 13 (2015) 325–334.
[45] S.A. Hamoudi, B. Hamdi, J. Brendlé, Tetracycline removal from water by adsorption on geomaterial, activated carbon and clay adsorbents, Ecol. Chem. Eng. S, 28 (2021) 303–328.

[46] A. Deb, M. Kanmani, A. Debnath, K.L. Bhowmik, B. Saha, Preparation and characterization of magnetic $CaFe_2O_4$ nanoparticles for efficient adsorption of toxic Congo Red dye from aqueous solution: predictive modelling by artificial neural network, Desal. Water Treat., 89 (2017) 197–209, doi: 10.5004/dwt.2017.21361.
[47] M.F. Abed, A.A.H. Faisal, Calcium/iron-layered double hydroxides - sodium alginate for removal of tetracycline antibiotic from aqueous solution, Alexandria Eng. J., 63 (2023) 127–142.
[48] Y. Wang, S. Gong, Y. Li, Z. Li, J. Fu, Adsorptive removal of tetracycline by sustainable ceramsite substrate from bentonite/red mud/pine sawdust, Sci. Rep., 10 (2020) 1–18.
[49] K.Y. Foo, B.H. Hameed, Insights into the modeling of adsorption isotherm systems, Chem. Eng. J., 156 (2010) 2–10.
[50] P.R. Puranik, J.M. Modak, K.M. Paknikar, A comparative study of the mass transfer kinetics of metal biosorption by microbial biomass, Hydrometallurgy, 52 (1999) 189–197.
[51] M.F. Al Juboury, M.H. Alshammari, M.R. Al-Juhaishi, L.A. Naji, A.A.H. Faisal, Mu. Naushad, E.C. Lima, Synthesis of composite sorbent for the treatment of aqueous solutions contaminated with methylene blue dye, Water Sci. Technol., 81 (2020) 1494–1506.
[52] S.S. Alquzweeni, R.S. Alkizwini, Removal of cadmium from contaminated water using coated chicken bones with double-layer hydroxide (Mg/Fe-LDH), Water, 12 (2020) 2303, doi: 10.3390/w12082303.
[53] T. Masinga, M. Moyo, V.E. Pakade, Removal of hexavalent chromium by polyethyleneimine impregnated activated carbon: intraparticle diffusion, kinetics and isotherms, J. Mater. Res. Technol., 18 (2022) 1333–1344.
[54] R. Bilas, K. Sriram, P.U. Maheswari, K.M.M. Sheriffa Begum, Highly biocompatible chitosan with super paramagnetic calcium ferrite ($CaFe_2O_4$) nanoparticle for the release of ampicillin, Int. J. Biol. Macromol., 97 (2017) 513–525.
[55] H.B. Lakshmi, B.J. Madhu, M. Veerabhadraswamy, Synthesis and characterization of nano-crystaline $CaFe_2O_4$ *via* solution combustion method from solid waste egg shells as source of calcium, Int. J. Eng. Res. Adv. Technol., 3 (2017) 21–30.
[56] F. Saedi, K. Hedayati, A facile synthesis and study of photocatalytic properties of magnetic $CaFe_2O_4$-CeO_2 nanocomposites applicable for separation of toxic azo dyes, J. Nanostruct., 10 (2020) 497–508.
[57] V. Oskoei, M.H. Dehghani, S. Nazmara, B. Heibati, M. Asif, I. Tyagi, S. Agarwal, V.K. Gupta, Removal of humic acid from aqueous solution using UV/ZnO nano-photocatalysis and adsorption, J. Mol. Liq., 213 (2016) 374–380.
[58] A.A.H. Faisal, L.A. Naji, Simulation of ammonia nitrogen removal from simulated wastewater by sorption onto waste foundry sand using artificial neural network, Assoc. Arab Univ. J. Eng. Sci., 26 (2019) 28–34.
[59] M. Ghaemi, G. Absalan, Fast removal and determination of doxycycline in water samples and honey by Fe_3O_4 magnetic nanoparticles, J. Iran. Chem. Soc., 12 (2015) 1–7.
[60] Z.T. Abd Ali, L.A. Naji, S.A.A.A.N. Almuktar, A.A.H. Faisal, S.N. Abed, M. Scholz, Mu. Naushad, T. Ahamad, Predominant mechanisms for the removal of nickel metal ion from aqueous solution using cement kiln dust, J. Water Process Eng., 33 (2020) 101033, doi: 10.1016/j.jwpe.2019.101033.
[61] H.K. Hami, R.F. Abbas, A.A. Waheb, D.A. Abdul abass, M.A. Abed, A.A. Maryoosh, Isotherm and pH effect studies of tetracycline drug removal from aqueous solution using cobalt oxide surface, Al-Nahrain J. Sci., 22 (2019) 12–18.
[62] G. Li, Q. Yuan, A.A. Khan, Effect of solution pH on the kinetic adsorption of tetracycline by la-modified magnetic bagasse biochar, Nat. Environ. Pollut. Technol., 18 (2019) 623–627.
[63] Y. Guo, W. Huang, B. Chen, Y. Zhao, D. Liu, Y. Sun, B. Gong, Removal of tetracycline from aqueous solution by MCM-41-zeolite A loaded nano zero valent iron: synthesis, characteristic, adsorption performance and mechanism, J. Hazard. Mater., 339 (2017) 22–32.
[64] N.P. Raval, M. Kumar, Development of novel core–shell impregnated polyuronate composite beads for an eco-efficient removal of arsenic, Bioresour. Technol., 364 (2022) 127918, doi: 10.1016/j.biortech.2022.127918.
[65] J.-P. Simonin, On the comparison of pseudo-first order and pseudo-second-order rate laws in the modeling of adsorption kinetics, Chem. Eng. J., 300 (2016) 254–263.
[66] A.A.H. Faisal, A.H. Shihab, Mu. Naushad, T. Ahamad, G. Sharma, K.M. Al-Sheetan, Green synthesis for novel sorbent of sand coated with (Ca/Al)-layered double hydroxide for the removal of toxic dye from aqueous environment, J. Environ. Chem. Eng., 9 (2021) 105342, doi: 10.1016/j.jece.2021.105342.
[67] Y. Lin, S. Xu, J. Li, Fast and highly efficient tetracyclines removal from environmental waters by graphene oxide functionalized magnetic particles, Chem. Eng. J., 225 (2013) 679–685.
[68] M. Ersan, U.A. Guler, U. Acıkel, M. Sarioglu, Synthesis of hydroxyapatite/clay and hydroxyapatite/pumice composites for tetracycline removal from aqueous solutions, Process Saf. Environ. Prot., 96 (2015) 22–32.
[69] J. Bao, Y. Zhu, S. Yuan, F. Wang, H. Tang, Z. Bao, H. Zhou, Y. Chen, Adsorption of tetracycline with reduced graphene oxide decorated with $MnFe_2O_4$ nanoparticles, Nanoscale Res. Lett., 13 (2018) 396, doi: 10.1186/s11671-018-2814-9.
[70] J. Lu, K. Xu, W. Li, D. Hao, L. Qiao, Removal of tetracycline antibiotics from aqueous solutions using easily regenerable pumice: batch and column study, Water Qual. Res. J., 53 (2018) 143–155.
[71] A. Huízar-Félix, C. Aguilar-Flores, A. Martínez-de-la Cruz, J. Barandiarán, S. Sepúlveda-Guzmán, R. Cruz-Silva, Removal of tetracycline pollutants by adsorption and magnetic separation using reduced graphene oxide decorated with α-Fe_2O_3 nanoparticles, Nanomaterials, 9 (2019) 313, doi: 10.3390/nano9030313.
[72] L.T. Popoola, Tetracycline and sulfamethoxazole adsorption onto nanomagnetic walnut shell-rice husk: isotherm, kinetic, mechanistic and thermodynamic studies, Int. J. Environ. Anal. Chem., 100 (2020) 1021–1043.
[73] A.A.H. Faisal, D.N. Ahmed, M. Rezakazemi, N. Sivarajasekar, G. Sharma, Cost-effective composite prepared from sewage sludge waste and cement kiln dust as permeable reactive barrier to remediate simulated groundwater polluted with tetracycline, J. Environ. Chem. Eng., 9 (2021) 105194, doi: 10.1016/j.jece.2021.105194.